

FLUCTUATION INDUCED CONDUCTIVITY OF SUPERCONDUCTORS
ABOVE THE TRANSITION TEMPERATURE: REGULARIZATION OF THE MAKI DIAGRAM

Joachim Keller and Victor Korenman

**CASE FILE
COPY**

Technical Report 72-016

July 1971



CENTER FOR THEORETICAL PHYSICS
OF THE
DEPARTMENT OF PHYSICS AND ASTRONOMY
UNIVERSITY OF MARYLAND
COLLEGE PARK, MARYLAND

This is a preprint of research carried out at the University of Maryland. In order to promote the active exchange of research results, individuals and groups at your institution are encouraged to send their preprints to

**PREPRINT LIBRARY
DEPARTMENT OF PHYSICS AND ASTRONOMY
UNIVERSITY OF MARYLAND
COLLEGE PARK, MARYLAND
20742
U.S.A.**

FLUCTUATION INDUCED CONDUCTIVITY OF SUPERCONDUCTORS
ABOVE THE TRANSITION TEMPERATURE: REGULARIZATION OF THE MAKI DIAGRAM*

Joachim Keller⁺ and Victor Korenman

Department of Physics and Astronomy and
the Center for Theoretical Physics
University of Maryland, College Park, Maryland 20742

The Maki contribution to the conductivity above the superconducting transition temperature is regularized within the framework of the BCS theory. This is achieved through the renormalization of the impurity scattering vertex by inclusion of the effects of pair fluctuations. The conductivity is evaluated for a thin film. It depends only on the reduced temperature and the normal resistance per square. Fair agreement is found with Al films over a wide temperature range. Agreement is not found with experiments on Bi, Pb and Ga films, which apparently contain a strong additional pair-breaking effect. The temperature range in which interactions among fluctuations become important in the Maki conductivity is generally larger than that given by the Ginzburg criterion.

I. INTRODUCTION

Many experiments on the electrical conductivity of superconducting thin films above the transition temperature¹ can be successfully described by a phenomenological theory of superconducting fluctuations² or an equivalent microscopic calculation by Aslamasov and Larkin³ (AL). According to this theory the excess conductivity σ' due to superconducting fluctuations above the transition temperature T_c of a thin film is given by the relation

$$\sigma' = \sigma'_{AL} = e^2/(16dt), \quad (1)$$

where t is the reduced temperature, $t = \ln(T/T_c) \approx (T - T_c)/T_c$ and d is the thickness of the film.

The AL theory is based on a diagrammatic expansion of the conductivity tensor in terms of independent fluctuations. Among the first order diagrams, all of which are required for gauge invariance, there are two which give rise to a strongly temperature dependent conductivity. One, generally called the AL diagram, leads to the expression in Eq. (1). The second, first discussed by Maki⁴ is shown in Fig. 1. The conductivity associated with this diagram in one and two dimensions is infinite for all temperatures above T_c .

This unphysical divergence is removed if a pair-breaking effect is present in the system⁵. In fact, recent experiments on aluminum films^{6,7} in the presence of a magnetic field are well described by a formula derived by Thompson⁵:

$$\sigma' = \sigma'_{AL} + \sigma'_{MT},$$

$$\sigma'_{MT} = (e^2/8d) \ln(t/\delta)/(t - \delta). \quad (2)$$

Here σ'_{MT} is the contribution to the electrical conductivity of the Maki diagram, and δ is the sum of the two pair-breaking parameters δ_H and δ_i , corresponding to the well known pair-breaking effect of the external magnetic field and an intrinsic pair-breaking mechanism respectively. In Eq. (2) t is defined as before but refers to the actual transition temperature T_c , which is related to the transition temperature T_{co} in the absence of pair-breaking effects by the relation $T_c = T_{co}(1 - \delta)$. In the case of aluminum films the intrinsic pair-breaking parameter δ_i which is treated as an adjustable parameter, is found to be proportional to the normal resistance per square R_{\square} ; numerically: $\delta_i \approx 5 \times 10^{-4} R_{\square}$, when R_{\square} is measured in Ω . The transition temperatures of these films, however, are strongly dependent on sample preparation so no systematic relation between resistivity and T_c has been observed.

Among the suggested origins of the intrinsic pair-breaking are⁸ a) proximity effects at the surface boundaries, b) the presence of localized magnetic moments, c) inelastic scattering of electrons by thermally excited phonons. In practice these effects may play an important role in reaching agreement with experiment. However it is unsatisfactory to be required to go outside the BCS model to achieve finite conductivity. If this were necessary it would be the first instance of a qualitative failure of the BCS theory.

We will show in this work, that the inclusion of the effect of superconducting fluctuations in the electron self energy and in the coherent scattering of an electron pair by impurities removes the divergence of the Maki diagram (and also of higher-order diagrams), and thus leads to a finite theory in the BCS model with no additional pair-breaking mechanism required.⁹

In the usual discussion of impure systems¹⁰ the scattering of normal electrons by randomly distributed fixed impurities is treated by including a finite lifetime in the momentum states of single electrons, and inserting vertex corrections to take account of the coherent scattering of two electrons. In the limit of small electron frequencies and small pair momentum these vertex corrections diverge. This divergence is related to the diffusive propagation of normal electrons in impure systems. The divergence of the Maki-diagram¹¹ Fig. 1 is a direct consequence of the diffusion poles of the two vertex functions associated with a superconducting fluctuation.

In the next section we will include the effects of superconducting fluctuations in the calculation of this vertex correction. We find, that its divergence is removed. In Section III this result is used in a recalculation of the contribution of the Maki diagram to the electrical conductivity. In this case the additional term in the denominator of the vertex function, which removes its divergence, acts like a pair-breaking effect. However, due to the strong dependence of this quantity on electron frequency and reduced temperature our result for the excess conductivity cannot be expressed by a Maki-Thompson formula Eq. (2), and also does not lead to a sizable shift of the transition temperature.

In a restricted temperature range above the transition temperature the contribution of the Maki-diagram to the conductivity of a thin film can be approximated by the function:

$$\sigma'_M = \frac{e^2}{8d} \left\{ \frac{1}{t - \delta_0} \frac{\delta_1}{\delta_1 - \delta_0} \ln \frac{t}{\delta_0} + \frac{1}{t - \delta_1} \frac{\delta_0}{\delta_0 - \delta_1} \ln \frac{t}{\delta_1} \right\}, \quad (4)$$

where δ_0 and δ_1 are given numerically by

$$\begin{aligned} \delta_0 &= 2.1 \times 10^{-5} R_{\square}/t, \\ \delta_1 &= 2.3 \times t. \end{aligned} \quad (5)$$

It should be noted that this contribution to σ' depends only on the reduced temperature and the normal resistance per square of the film, and contains no adjustable parameters.

In Section IV we compare the present theory with measurements of the electrical conductivity of thin aluminum films. While our results agree relatively well with experiments at temperatures close to the transition temperature, systematic deviations are found at higher temperatures. An additional correction which improves the agreement will also be discussed in this section.

Our theory does not agree at all with experiments on highly disordered bismuth, lead and gallium films where no contribution of the Maki-diagram is observed.¹ This discrepancy apparently cannot be resolved within the frame-work of the present theory, because all our results in two dimensions depend only on the normal resistance

per square and the reduced temperature. Thus all thin films with equal resistance per square should have a similar electrical conductivity as function of the reduced temperature. The origin of this discrepancy may lie in the strong coupling nature of these materials.

Our results differ from those of Takayama and Maki¹² who sum the contributions of a whole class of diagrams including a finite pair-breaking effect and keeping only the most divergent diagrams in each order. Their final result still diverges when the pair-breaking parameter is set equal to zero.

We also disagree with the recent work of Schmid¹³ who uses an alternate method for treating impure electron systems. He concludes that there is no sizable contribution of the Maki term to the conductivity even in the absence of pair-breaking effects. However, we find that his method leads to a finite value of the Meissner current above T_c . Furthermore, Schmid cites no reason for the failure of the usual treatment of impurity scattering in this case.

II. CORRECTIONS TO THE PAIR VERTEX FUNCTION

In the following calculation of the pair vertex function in the presence of superconducting fluctuations extensive use is made of an expansion in terms of independent fluctuations.^{12,14} By this we mean the following: We represent the effect of the repeated interaction of a pair of electrons via the BCS potential by a fluctuation propagator $K(\vec{q}, \omega_s)$, which also includes the effect of scattering by randomly distributed impurities in intermediate states. In diagrams fluctuations are represented by wavy lines and can be treated for-

mally like phonon propagators. Each interaction of a single electron state with a superconducting fluctuation involves an integration over the fluctuation four-momentum (\vec{q}, ω_s) . Two fluctuations are called independent, if they contain different four-momenta as independent integration variables. The order of a diagram in terms of independent fluctuations is then defined by the number of independent fluctuation integrals. In a two dimensional system this is equal to the number of factors $1/d$, which appear in the corresponding analytic expression.

As only contributions from fluctuations with $\omega_s = 0$, or $\omega_s \rightarrow 0$ in an analytic continuation, become singular when $T \rightarrow T_c$, it is possible to split up a sum over fluctuation frequencies into a singular contribution¹⁵ and a non singular part, which depends only weakly on temperature.

In this section we will consider only the singular contributions due to superconducting fluctuations. Some of these approximations will be examined in more detail in Section IV.

In the absence of fluctuation effects the electron propagator of momentum \vec{p} and discrete frequency $i\omega_n$ is given by

$$G_0(\vec{p}, \omega_n) = (i\tilde{\omega}_n - \zeta_p)^{-1} \quad (6)$$

$$\tilde{\omega}_n = \omega_n + (1/2\tau_0) \text{sign}(\omega_n).$$

The vertex correction associated with a pair of electrons with nearly opposite momenta \vec{p}_1 and \vec{p}_2 and small frequencies ω_1, ω_2

is

$$\Lambda_0(\omega_1, \omega_2; q = |\vec{p}_1 + \vec{p}_2|) = \begin{cases} |\tilde{\omega}_1 - \tilde{\omega}_2| \times (|\omega_1 - \omega_2| + Dq^2)^{-1}, & \omega_1 \omega_2 < 0 \\ 1 & , \omega_1 \omega_2 > 0 \end{cases} \quad (7)$$

The fluctuation propagator is

$$K_0(\vec{q}, \omega_s) = - (8T/N(0)\pi) \times (|\omega_s| + Dq^2 + \varepsilon)^{-1}. \quad (8)$$

In the above expressions, $\omega_n = (2n + 1)\pi T$, $\omega_s = 2s\pi T$, ζ_p is the kinetic energy of an electron with momentum \vec{p} , measured from the Fermi energy, τ_0 is the lifetime of electrons due to impurity scattering, D is the diffusion constant, $N(0)$ is the density of electron states of one spin at the Fermi energy, and $\varepsilon = (8T/\pi) \cdot t$. The expressions for Λ_0 and K_0 are appropriate for dirty superconductors with $\tau_0 T \ll 1$. If we neglect the momentum dependence of the impurity scattering potential U , then the scattering rate τ_0^{-1} and the diffusion constant D are given in Born approximation by

$$\begin{aligned} \tau_0^{-1} &= 2\pi N(0)nU^2, \\ D &= v_F^2 \tau_0 / 3 \end{aligned} \quad (9)$$

Here n is the density of impurities and v_F the velocity of electrons at the Fermi energy.

In the presence of superconducting fluctuations, corrections are required both to the single electron propagator G and the vertex function Λ . The renormalized vertex function is found from the integral equation whose diagrammatic representation is given in Fig. 2. In the kernel of the integral equation we have retained only diagrams

which are of first order in superconducting fluctuations, but we have included all the terms which make an important contribution to the vertex. These are the terms which are singular for $T \rightarrow T_c$ and which involve no restrictions on the momentum transfer in an impurity scattering event (no crossing diagrams). The restriction to first order terms is a valid approximation when the fluctuation corrections are small. Of course it fails when the transition temperature is approached too closely.

To the same approximation it is sufficient to use unrenormalized propagators and vertex functions in a calculation of the self-energy contributions due to fluctuations in diagram a and the correction to the impurity scattering in diagram b of Fig. 2.

One of the self energy terms, first calculated by Abrahams, Redi and Woo¹⁶, depends on the momentum of the electron state. In a similar way the renormalized vertex depends on the momenta of the incoming and outgoing electron states. It can be conveniently written as

$$\Lambda(\omega_1, \omega_2; \vec{p}_1, \vec{p}_2) = a(\omega_1, \omega_2; q) + b(\omega_1, \omega_2; \vec{p}_1, \vec{p}_2), \quad (10)$$

where the functions a and b correspond to the diagrams a and b in Fig. 2.

Using again the assumption made above that the corrections due to superconducting fluctuations are small the integral equation for the vertex function can be simplified considerably: As diagram b of Fig. 2 already contains first-order contributions of fluctuations explicitly we can in its evaluation replace the complete vertex

function Λ by its momentum independent part $a(\omega_1, \omega_2; q)$. In diagram a the complete vertex function has to be used. This leads to an equation for a similar to that represented by Fig. 2, except that diagram b is closed by an additional impurity line. A discussion of this derivation and details of the evaluation of the diagrams needed to solve this equation are presented in Appendix A.

The final result for the momentum independent part a of the vertex function, which determines the analytic behavior of the complete vertex function for small frequencies and small pair momentum, is rather simple. Keeping only the singular contributions due to fluctuations we get

$$a(\omega_1, \omega_2; q) = |\tilde{\omega}_1 - \tilde{\omega}_2| \times \{ (|\omega_1 - \omega_2| + Dq^2)(1 + M(|\omega_1|) + M(|\omega_2|)) + L(|\omega_1|) + L(|\omega_2|) \}^{-1}, \quad (11)$$

where

$$L(|\omega_n|) = -\tau_0^2 T \sum_{0 \leq \omega_s' < |\omega_n|} \sum_{\vec{q}'} K_0(\vec{q}', \omega_s') \Lambda_0^2(|\omega_n|, \omega_s' - |\omega_n|; \vec{q}') \times (2|\omega_n| - \omega_s' + Dq'^2) \quad (12)$$

$$\approx (8T^2/N(0)\pi) \sum_{\vec{q}'} [(Dq'^2 + \epsilon)(|2\omega_n| + 2Dq'^2 + \epsilon)]^{-1}.$$

Using the same type of approximation the function M can be expressed

by

$$M(|\omega_n|) = -\frac{1}{2} \partial L(|\omega_n|) / \partial |\omega_n|. \quad (13)$$

In the final expression of Eq. 12 the analytic continuation with respect to the frequency ω_n can be easily done by replacing $|\omega_n|$

by $-\omega$ sign (ω_n). Its derivation is not entirely trivial, but can be done by methods similar to those used in Ref. 14 and 16.

The function L which removes the divergence of the vertex function at zero frequencies ω_1, ω_2 and zero pair momentum q is related but not equal to the self-energy contribution due to fluctuations¹⁶. The extra factor $(2|\omega_n| - \omega_s' + Dq'^2)$ in the integrand of Eq. (12) comes from an expansion of electron Green's functions with respect to the frequency and momentum of fluctuations. It is only the inelastic part of the interaction with superconducting fluctuations, changing the momentum and frequency of the single electron states, which contributes to the "pair-breaking" function L . The contribution to the vertex equation from the self energy terms of diagram a is cancelled by the term from diagram b, when electron momentum and frequency changes are ignored.

The function M can be regarded as a correction to the coefficient of the dynamical quantity $(|\omega_1 - \omega_2| + Dq^2)$. It is important only at finite frequencies or finite pair momentum. We want to notice that the derivation of this coefficient is not complete, because in the simplified version of the integral equation, we have left out systematically factors of the order $(1 + M)$. As in the calculation of the Maki diagram the value of the vertex function in the limit of small frequencies and small pair momentum is most important we will neglect such corrections in the following. The pair-breaking function L is given in 1,2 and 3 dimensions by

$$L_1(|\omega_n|) = \frac{4T^2\xi}{N(0)d^2D\pi} \frac{1}{\epsilon - 2|\omega_n|} \left[\left(\frac{2\epsilon}{\epsilon + 2|\omega_n|} \right)^{1/2} - 1 \right], \quad (14)$$

$$L_2(|\omega_n|) = \frac{2T^2}{N(0)dD\pi^2} \frac{1}{\epsilon - 2|\omega_n|} \ln \left(\frac{2\epsilon}{\epsilon + 2|\omega_n|} \right), \quad (15)$$

$$L_3(|\omega_n|) = \frac{2T^2}{N(0)\xi D\pi^2} \frac{1}{\epsilon - 2|\omega_n|} \left(1 - \left(\frac{\epsilon + 2|\omega_n|}{2\epsilon} \right)^{1/2} \right), \quad (16)$$

where ξ is the GL coherence length, $\xi(t) = (D/\epsilon)^{1/2}$.

In a calculation of the renormalized fluctuation propagator and the AL diagram the vertex function Λ enters only at finite discrete frequencies $|\omega_n| \geq \pi T$. Here the value of L is very small, and leads only to a slight shift in the transition temperature, which will be neglected in the present context.

III. CALCULATION OF THE MAKI DIAGRAM

The contribution of the Maki diagram shown in Fig. 1 to the conductivity tensor $Q_{\alpha\beta}^M(0, \omega_0)$ which relates the induced electrical current density to a transverse vector potential with discrete frequency $\omega_0 > 0$, is given by

$$\begin{aligned} Q_{\alpha\beta}^M(0, \omega_0) &= (2e^2 T^2 / m^2) \sum_{\omega_n, \omega_s} \sum_{\vec{p}, \vec{q}} p_\alpha (q - p)_\beta \\ &\times G(\vec{p}, \omega_n) G(\vec{p}, \omega_n - \omega_0) G(\vec{q} - \vec{p}, \omega_s - \omega_n) G(\vec{q} - \vec{p}, \omega_0 + \omega_s - \omega_n) \\ &\times \Lambda(\omega_n, \omega_s - \omega_n; q) \Lambda(\omega_n - \omega_0, \omega_0 + \omega_s - \omega_n; q) K(\vec{q}, \omega_s). \end{aligned} \quad (17)$$

The singular¹⁵ contribution of the right-hand side of Eq. (17) comes from terms with frequencies $\omega_s = 0$, $0 < \omega_n < \omega_0$, and small pair momentum \vec{q} . The singular terms give the most important contribution near the transition temperature. In the following we will consider only

these terms and will neglect the dependence of the electron propagators on the pair momentum \vec{q} . As long as we are not too close to T_c , however, the corrections due to fluctuations are still small and can be neglected everywhere but in the denominator of the vertex functions Λ .

With these approximations the integration over the momentum \vec{p} of the electron states can be carried out easily and gives

$$Q_{\alpha\beta}^M(0, \omega_0) = \delta_{\alpha\beta} 16 e^2 D T^2 \sum_{\vec{q}} P(\vec{q}, \omega_0) \times (\epsilon + Dq^2)^{-1}, \quad (18)$$

where

$$P(\vec{q}, \omega_0) = T \int_{0 < \omega_n < \omega_0} [(\omega_n + Dq^2/2 + L(\omega_n))(\omega_0 - \omega_n + Dq^2/2 + L(\omega_0 - \omega_n))]^{-1}. \quad (19)$$

As the static conductivity σ' is obtained by taking the limit

$$\sigma' = \lim_{\omega_0 \rightarrow +0} Q(0, \omega_0) / \omega_0 \quad (20)$$

the function $P(\vec{q}, \omega_0)$ has to be calculated as an analytic function of the variable ω_0 in the limit of small frequencies.

If we neglect the dependence of the pair-breaking function L on frequency, taking its value at $\omega_n = 0$ as a pair-breaking parameter, we obtain in the limit of small values of Dq^2 and ω_0

$$P(\vec{q}, \omega_0) = (\omega_0/4T)(Dq^2 + 2L(0))^{-1}. \quad (21)$$

In the case of a thin film this expression leads to a Maki-Thompson type formula, Eq. (2), for the excess conductivity with a temperature dependent pair-breaking parameter δ_0 given by

$$\delta_0 = (\pi/4T)L(0) = (\ln 2/16t)(N(0)dD)^{-1}. \quad (22)$$

Corresponding expressions in 1 and 3 dimensions are easily obtained using Eqs. (14) and (16). In order to take account of the decrease of the pair-breaking function L with increasing frequency, we have approximated L as given in Eq. (15) by the two-parameter expression

$$L(|\omega_n|) \approx \alpha/(\beta + |\omega_n|) \quad (23)$$

Then, using the same approximations as in the derivation of Eq. (21), we find

$$P(q, \omega_0) = \frac{\omega_0}{4T} \left\{ \frac{1}{Dq^2 + 2\alpha/\beta} + \frac{2\alpha/\beta}{(Dq^2 + 2\alpha/\beta)(Dq^2 + 2\beta)} \right\}. \quad (24)$$

As the frequency dependence of L is most important for frequencies in the range $0 < |\omega_n| < \epsilon$, we have determined the coefficients α and β by equating the values and first derivatives of both sides of Eq. (23) at $\omega_n = 0$. Then the contribution of the Maki diagram to the electrical conductivity is given by Eq. (4) with

$$\delta_1 = \frac{\pi}{4T} \beta = - \frac{\pi}{4T} \frac{L(0)}{\partial L(0)/\partial |\omega_n|} = \frac{\ln 2}{1 - \ln 2} \cdot t. \quad (25)$$

The numerical expression for δ_0 given in the introduction is obtained by using the numerical relation

$$(N(0)dD)^{-1} = 4.86 \times 10^{-4} R_{\square}, \quad (26)$$

where R_{\square} is measured in Ω .

As can be seen from Eq. (4) the correction due to the additional parameter δ_1 is significant only at temperatures sufficiently close to the transition temperature. It is just in this temperature range, however, that correction factors of the order $(1 + M)$ become impor-

tant in the vertex function. In this view, the precise form of the temperature dependence of the conductivity as given by Eq. (4) should not be considered accurate at temperatures too close to the transition temperature. In the following we use Eq. (4) as an extrapolation formula to small reduced temperatures.

The range of validity of Eq. (4) will be discussed more carefully in the next section.

IV. COMPARISON WITH EXPERIMENT

In Fig. 4 we have compared our theoretical result for the excess conductivity due to superconducting fluctuations with measurements on two aluminum films^{6,7} with different values for the normal resistance per square. We have plotted the ratio σ_n/σ' of the conductivity σ_n in the normal state, $\sigma_n = 2e^2N(0)D$, and the excess conductivity σ' given by Eq. (4) as a function of the reduced temperature $(T - T_c)/T_c$. For comparison the results of the AL theory are also shown. In view of the fact that we don't use any adjustable parameter the agreement with the experimental data is quite satisfactory near the transition temperature. However, systematic deviations are found at higher temperatures, which are due to the decrease of the pair-breaking parameter δ_0 with increasing temperature.

This raises the question of the validity of the different approximations used. Basically we have applied two different kinds of approximations, which restrict the accuracy of our results both at temperatures close to the transition temperature and at high temperatures. In fact, these approximations have been widely used

in previous calculations of superconducting properties above the transition temperature, but their implications are more drastic in the present case.

Our assumption that the contribution of fluctuations is small in the vertex functions used in the calculation of the Maki diagram is equivalent to the condition $M(\omega_n \rightarrow 0) < 1$. Using Eqs. (13), (15) and (26) this gives the requirement $t^2 > 10^{-4} R_D$. Corrections to other expressions, such as the fluctuation propagator and the AL conductivity, are not important as long as the pair-breaking effect at finite frequencies is small compared to the reduced temperature, $L(\omega_n = \pi T)/T < t$. For a thin film this is fulfilled for $t > 10^{-4} R_D$.

This latter condition agrees with the Ginzburg¹⁷ criterion for the critical region, which has been discussed by several authors.¹⁸ However, the first condition, which in most cases is far more stringent, is clearly violated when $t < 0.1$ for the aluminum film with $R_D \approx 129$. Here the good agreement between theory and experiment for this film may be accidental.

We have, in addition, restricted our attention to the singular terms in σ_M' and L , those arising from fluctuations with $\omega_s = 0$. Contributions from terms with nonzero values of ω_s become comparable in size at higher temperatures, when $t \sim \pi/8$. In principle these terms should be included in any discussion of the properties of a superconductor somewhat above T_c . In the calculation of the Maki conductivity it is particularly important to include these terms

because they would diverge in the absence of pair-breaking. In the present theory the pair-breaking strength becomes small at high temperatures giving a large temperature dependent effect.

It is difficult to accurately evaluate the pair-breaking function $L(\omega_n)$ in this temperature range, because the additional terms, mentioned above, here depend on high momentum and high frequency cutoffs.

As a rough estimate of the effects of these terms we have computed the conductivity by summing the non singular contribution while neglecting the frequency dependence of $L(\omega_n)$ in the vertex function. In particular we have evaluated numerically the sums in Eq. (17) in the frequency range $\omega_0 > \omega_n > 0$, $\omega_n > \omega_s > \omega_n - \omega_0$. It is only in this frequency range that the poles of the vertex functions "pinch" and lead to a divergent contribution to the conductivity in one and two dimensions. Furthermore, we have taken for $L(\omega_n)$ its value at zero frequency $L(0) = 4T \delta_0(t)/\pi$ (See Eq. (22)). An expression for the conductivity suitable for numerical evaluation is given in Appendix B. Results are shown in Fig. 4. Much of the deviation of theory from experiment has been removed at high temperatures.

V. DISCUSSION

We have regularized the Maki conductivity within the context of the BCS model by removing the divergence of the impurity scattering pair-vertex function. It is worthwhile to examine if the renormalization of this vertex is merely an artifact of our approximation scheme. Indeed, in the absence of interactions other than with impurities, time reversal connects the pair vertex with the particle-hole (p-h) vertex while particle conservation requires a divergence of the latter at small momentum and frequency. This connection between the vertices no longer holds in the presence of pair fluctuations. Corrections to the two vertices are quite different. The p-h vertex has first order corrections given by AL and Maki diagrams, as well as those shown in Fig. 2. It is not in contradiction with the requirements of gauge invariance and time reversibility that the divergence of the pair vertex is removed. We can construct explicitly gauge invariant approximations, for example by dropping diagram b of Fig. 2 and using fully renormalized propagators and vertex functions everywhere. Then the divergence of the pair vertex is removed again, giving a much stronger pair breaking than in the present case. The results of this otherwise consistent theory are wrong, however, because of an incomplete treatment of the impurity interactions.

In the present theory we have kept higher order fluctuation corrections only where they are needed to remove a divergence in the conductivity. In the extension to a gauge invariant formulation additional terms are surely required. We believe they have a small effect in the transverse gauge at temperatures not too close to T_c . In this calculation we have attempted to ensure a consistent treatment of impurity interactions by keeping all important first order terms in the kernel of the vertex equation. The order

of a term is a valid concept because of the existence of the formal expansion parameter associated with fluctuations, $1/d$ for two dimensional systems. The pair-breaking effect we have found in first order cannot be cancelled by higher order terms.

Now in the presence of a magnetic field, the superconducting transition temperature is reduced and the divergence of the pair vertex is removed, even in the absence of fluctuations. It is well known that a spatial variation of the static order parameter in a dirty superconductor acts like a pair-breaking mechanism in similarly modifying the electron system to suppress superconductivity.¹⁹ In this context we recall that our vertex remains divergent when the change of momentum and frequency of an electron interacting with a fluctuation is ignored. In our calculation the pair-breaking is caused by the known interaction $\tau_0 v_F \hat{p} \cdot \vec{q}$ associated with a spatially varying fluctuation¹⁹ and the additional pair-breaking interaction $\tau_0 \omega_S$ related to its time variation. (\hat{p} is an electron momentum unit vector.)

The manner in which superconducting fluctuations enter the vertex function demonstrates that an expansion of the conductivity tensor in terms of fluctuations is only possible when it is followed by a resummation of an infinite number of fluctuation contributions. It is not surprising that the Ginzburg criterion for the critical region which arises from a theory based on an expansion in the order parameter is inapplicable in just those expressions where a simple expansion is not allowed.

The present theory applies primarily to materials whose superconducting properties can be described by the BCS model, and is in relatively good agreement with experiments on aluminum films. For films of Pb, Bi, and Ga, however, a much larger pair-breaking effect is required to account for the observed suppression of the Maki conductivity. In these presumably strong coupling materials the inelastic interactions between electrons and phonons

could produce a large pair-breaking effect, either through the retardation of the effective electron-electron interaction or the scattering of electrons from thermal phonons. Other pair-breaking mechanisms like the proximity effect may also play an important role. Furthermore, the pair-breaking effect due to fluctuations may be greatly enhanced by the strong-coupling nature of these materials.

Acknowledgements

One of us (JK) would like to thank Bruce Patton for describing to him some of his work on this subject. Dr. Patton informs us that he has reached conclusions similar to ours in his thesis, submitted to Cornell University in the Spring of 1971.

Appendix A

The equation for Λ can be written

$$\Lambda = 1 + K_1\Lambda + K_2\Lambda = a + b, \quad A1$$

where K_1 and K_2 are integral operators associated with diagrams a and b in Fig. 2, respectively. K_1 produces the momentum independent part of Λ and K_2 the momentum dependent part. Then

$$a = 1 + K_1\Lambda = 1 + K_1a + K_1b, \quad A2$$

$$b = K_2\Lambda = K_2a + K_2b,$$

which have the formal solution

$$b = (1 - K_2)^{-1} K_2a,$$

$$a = [1 - K_1 - K_1(1 - K_2)^{-1} K_2]^{-1}.$$

Now K_2 is of first order in fluctuations while K_1 has a zero order part as well. Then, to first order

$$b = K_2a \quad A3$$

$$a = [1 - K_1 - K_1K_2]^{-1} \quad A4$$

where the zero order part of K_1 has to be used in the expression K_1K_2 . The next terms omitted in this approximation give a correction factor of order $1 + M$.

Since a is momentum independent, the momentum sums implied by the operators K_1 and K_2 can be performed, giving an algebraic equation for a .

$$a = [1 - V_0 - (V_1 + V_2 + V_3) - (V_1^x + V_2^x + V_3^x)]^{-1}. \quad A5$$

Here $V_0 - V_3$ correspond to the different diagrams of Fig. 2, while $V_1^x - V_3^x$ correspond to diagrams where the fluctuation propagator is associated with the other electron line. They are related to the operators K_1 and K_2 by

$$K_1 \rightarrow V_0 + V_1 + V_2 + V_1^x + V_2^x ,$$

$$K_1 K_2 \rightarrow V_3 + V_3^x .$$

Explicitly:

$$V_0 = nU^2 \sum_{\vec{p}} G_0(\vec{p} + \vec{q}/2, \omega_1) G_0(-\vec{p} + \vec{q}/2, \omega_2),$$

$$V_1 = nU^2 \sum_{\vec{p}} G_0^2(\vec{p} + \vec{q}/2, \omega_1) G_0(-\vec{p} + \vec{q}/2, \omega_2) \sum_1^f(\vec{p} + \vec{q}/2, \omega_1),$$

$$V_2 = nU^2 \sum_{\vec{p}} G_0^2(\vec{p} + \vec{q}/2, \omega_1) G_0(-\vec{p} + \vec{q}/2, \omega_2) \sum_1^i(\omega_1),$$

$$V_3 = (nU^2)^2 \sum_{\vec{p}} \sum_{\vec{p}'} G_0(\vec{p} + \vec{q}/2, \omega_1) G_0(-\vec{p} + \vec{q}/2, \omega_2) G_0(\vec{p}' + \vec{q}/2, \omega_1)$$

$$\times G_0(-\vec{p}' + \vec{q}/2, \omega_2) T \sum_{\omega_s'} \sum_{\vec{q}'} K_0(\vec{q}', \omega_s') \Lambda_0^2(\omega_1, \omega_s' - \omega_1, \vec{q}')$$

$$\times G_0(\vec{q}' - \vec{p} - \vec{q}/2, \omega_s' - \omega_1) G_0(\vec{q}' - \vec{p}' - \vec{q}/2, \omega_s' - \omega_1). \quad A6$$

where

$$\sum_1^f(\vec{p}, \omega_n) = T \sum_{\omega_s'} \sum_{\vec{q}'} K_0(\vec{q}', \omega_s') \Lambda_0^2(\omega_n, \omega_s' - \omega_n, \vec{q}') G_0(\vec{q}' - \vec{p}, \omega_s' - \omega_n)$$

$$\sum_1^i(\omega_n) = nU^2 \sum_{\vec{p}} G_0^2(\vec{p}, \omega_n) \sum_1^f(\vec{p}, \omega_n)$$

and $V_1^x - V_3^x$ are obtained from $V_1 - V_3$ by the replacement $\omega_1, \omega_2 \rightarrow -\omega_2, -\omega_1$.

To simplify notation we set $\omega_1 > 0, \omega_2 < 0$. The singular part of the frequency sum in V_1 comes from the range $0 \leq \omega_s' < \omega_1$. The momentum sums

are easily performed using the standard approximation for the momentum dependence of the kinetic energy near the Fermi surface and expanding all electron propagators to second order in powers of $(\omega'_s - \omega_s)$, $(\hat{p} \cdot \vec{q}) v_F$ and $\hat{p} \cdot (\vec{q}' - \vec{q}) v_F$. Here \hat{p} is a vector of unit length, and $\omega_s = \omega_1 + \omega_2$. Then

$$V_0 = \tilde{\Omega}^{-1} [\tau_0^{-1} - Dq^2] \quad A7$$

$$V_1 = (\tilde{\Omega}^3 \tau_0)^{-1} \sum_{\omega_1} \{2 + \tau_0 [3(\omega'_s - \omega_s) - 4Dq'^2 - 4Dq^2]\}$$

$$V_2 = -(\tilde{\Omega}^3 \tau_0)^{-1} \sum_{\omega_1} \{1 - \tau_0 (\omega_1 - \omega_2) + \tau_0 [2(\omega'_s - \omega_s) - 3Dq'^2 - 3Dq^2]\}$$

$$V_3 = -(\tilde{\Omega}^3 \tau_0)^{-1} \sum_{\omega_1} \{1 - \tau_0 (\omega_1 - \omega_2) + \tau_0 [2(\omega'_s - \omega_s) - 2Dq'^2 - 2Dq^2]\}.$$

Here $\tilde{\Omega} = \tilde{\omega}_1 - \tilde{\omega}_2 = \omega_1 - \omega_2 + \tau_0^{-1}$ and we have defined the summation operator

$$\sum_{\omega_1} f(\vec{q}', \omega'_s) \equiv T \sum_{0 < \omega'_s < \omega_1} \sum_{\vec{q}'} K_0(\vec{q}', \omega'_s) \Lambda_0^2(\omega_1, \omega'_s - \omega_1, \vec{q}') f(\vec{q}', \omega'_s).$$

The terms proportional to $\tau_0 (\omega_1 - \omega_2)$ in V_1 and V_2 came from expansion of a factor of $(\tau_0 \tilde{\Omega})^{-1}$.

We note that in the sum $V_1 + V_2 + V_3$ the leading contributions due to fluctuations cancel one another. Then the solution of Eq. (A5) is given by Eq. (11) of Section (II).

Appendix B

If we include contributions from fluctuations with finite frequencies ω_s in the calculation of the Maki diagram, the expression for the conductivity tensor Eq. (18) is replaced by

$$Q_{\alpha\beta}^M(0, \omega_0) = \delta_{\alpha\beta} 64e^2DT^3 \sum_{\omega_s, \omega_n} \sum_{\vec{q}} [(|\omega_s| + Dq^2 + \epsilon) \times (|2\omega_n - \omega_s| + Dq^2 + 2L)(|2\omega_0 + \omega_s - 2\omega_n| + Dq^2 + 2L)]^{-1}. \quad B1$$

As indicated in Section IV the frequency sums are restricted to the range $\omega_0 > \omega_n > 0$ and $\omega_n > \omega_s > \omega_n - \omega_0$. We recall that ω_n is a Fermi frequency (odd) while ω_s and ω_0 are boson frequencies (even). In Eq. (B1) we have already neglected the frequency dependence of the pair-breaking function and have replaced L by its value at zero frequency, $L = (4T/\pi)\delta_0(t)$.

Before the frequency sums can be carried out numerically we have to convert the sums into expressions which allow an analytic continuation with respect to ω_0 . This can be done in many different ways leading to a variety of final expressions. We found it convenient to replace each restricted sum by the difference of two infinite sums over positive frequencies, changing variables where necessary to avoid poles in the unphysical sheet. Finally we take the limit $\omega_0 \rightarrow 0$. By this procedure we find for the Maki conductivity

$$\sigma_M' = 128 e^2DT^3 \sum_{\omega_n > 0} \sum_{\vec{q}} d^{-1} \{ e^{-1}(2\omega_n + d)^{-2} + \sum_{\omega_s > 0} [(\omega_s + e)^{-1} (2\omega_n + \omega_s + d)^{-2} + (2\omega_n + \omega_s + d)^{-1} (\omega_s + e)^{-2} - (2\omega_n + d + e)^{-1} (2\omega_n + \omega_s - 2\bar{\omega} + d)^{-2} - (2\omega_n + d + e)^{-1} (\omega_s + e)^{-2}] \}. \quad B2$$

Here $\bar{\omega} = \pi T$ while e and d depend on the pair momentum q according to

$$e = Dq^2 + \epsilon,$$

$$d = Dq^2 + 2L.$$

The first term in the curly brackets leads to a Maki-Thompson type formula for the conductivity and gives the major contribution near T_c . We note that the additional terms would also diverge in 1 and 2 dimensions in the absence of pair breaking because of the common prefactor d^{-1} . At higher temperatures they reduce considerably the contribution from the first term. We have calculated the right hand side of Eq. (B2) by first performing the momentum integration analytically and then calculating the sums numerically.

References and Notes

* Work supported in part by the Army Research Office, Durham, the Office of Naval Research, and by the Deutsche Forschungsgemeinschaft. Computer time for this project was supported by NASA Grant NsG-398 to the Computer Science Center of the University of Maryland.

† Present address: Fachbereich Physik, Universität Regensburg, Germany.

1. R. E. Glover, III, Phys. Lett. 25A, 542 (1967); D. G. Naugle and R. E. Glover, Phys. Lett. 28A, 110 (1969); R. E. Glover in "Proceedings of the International Conference on the Science of Superconductivity," Stanford, 1969 (unpublished).
2. E. Abrahams and J. W. F. Woo, Phys. Lett. 27A, 117 (1968); A. Schmid, Z. Physik 215, 210 (1968); H. Schmidt, Z. Physik 216, 336 (1968).
3. L. G. Aslamazov and A. I. Larkin, Phys. Lett. 26A, 238 (1968); Fiz. Tverd. Tela 10, 1104 (1968) [English translation: Sov. Phys. - Solid State 10, 875 (1968)].
4. H. Maki, Progr. Theor. Phys. 40, 193 (1968).
5. R. S. Thompson, Phys. Rev. B1, 327 (1970).
6. J. E. Crow, R. S. Thompson, M. A. Klenin, and A. K. Bhatnagar, Phys. Rev. Lett. 24, 371 (1970).
7. K. Kajimura and N. Mikoshiba, preprint.
8. The influence of these effects is discussed, for instance, in Ref. 7.
9. An outline of this calculation has been submitted to Phys. Rev. Letters.
10. See, for instance, A. A. Abrikosov, L. P. Gorkov, and I. Ye. Dzyaloshinskii, Quantum Field Theoretical Methods in Statistical Physics, Pergamon Press, Oxford (1965).

11. By "divergence of the Maki diagram" we mean "divergence of the contribution of the Maki diagram to the electrical conductivity in 1 and 2 dimensional superconductors above the transition temperature.
12. H. Takayama and K. Maki, preprint.
13. A. Schmid, Z. Physik 243, 346 (1971).
14. J. P. Hurault and K. Maki, Phys. Rev. B2, 2560 (1970).
15. We use the word "singular" to refer to expressions which become infinite only at the transition temperature and the word "divergent" to refer to expressions which are infinite for some values of momentum or frequency at all temperatures in the absence of pair-breaking.
16. A. Abrahams, M. Redi, J. W. F. Woo, Phys. Rev. B1, 208 (1970).
17. V. L. Ginzburg, Fiz. Tverd. Tela 2, 2031 (1960) [English translation: Sov. Phys. - Solid State 2, 1824 (1960)].
18. For a review paper on the breakdown of the mean field theory, see P. C. Hohenberg in "Proceedings of the Conference on Fluctuations in Superconductors," edited by W. S. Goree and F. Chilton (Stanford, Calif., 1968), p. 305.
19. For a compilation and discussion of pair-breaking effects in dirty superconductors, see K. Maki in "Superconductivity," edited by R. D. Parks (Marcel Dekker, Inc., New York, 1969); Vol. 2, p. 1035.

Figure Captions

- Fig. 1 - Maki diagram. The two vertex corrections (broken lines) associated with the fluctuation propagator (wavy line) are responsible for the divergence of the electrical conductivity from this diagram.
- Fig. 2 - Diagrammatic representation of the integral equation for the renormalized vertex function $\Lambda(\omega_1, \omega_2; p_1, p_2)$. Broken lines denote impurity scattering, wavy lines are pair fluctuations, and solid lines are electron propagators whose self energy contains the impurity scattering, but not fluctuations.
- Fig. 3 - The inverse of the excess conductivity σ' , normalized to the conductivity σ_n of the normal state, for two aluminum films. Solid curves are calculated from Eq. (4), experimental points are taken from Ref. 6 and 7 for the films with $R_{\square} = 3.31 \Omega$ and $R_{\square} = 129.12 \Omega$, respectively. The lines labelled AL have the slopes predicted by the AL theory, Eq. (1).
- Fig. 4 - The inverse of the excess conductivity for the high resistance film presented in Fig. 3 over an extended temperature range. Curve a is calculated from Eq. (4), curve b contains corrections from fluctuation with finite frequencies and is calculated from Eq. (B2).

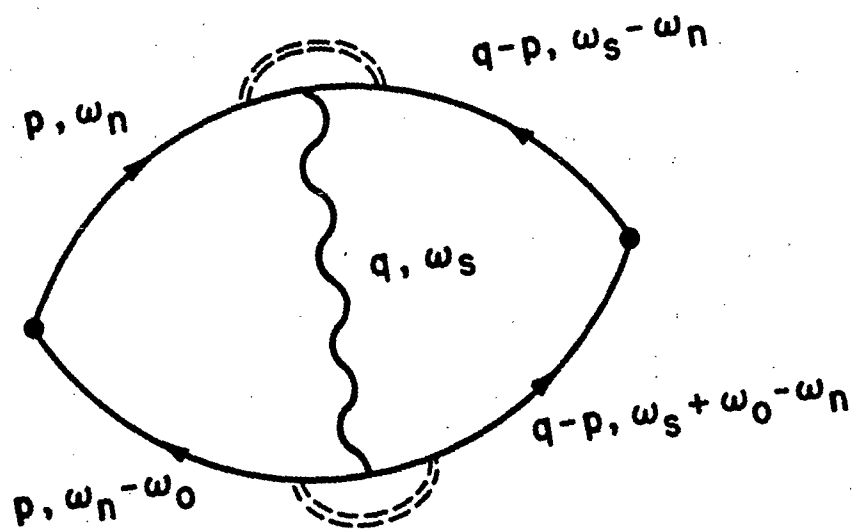


Fig. 1

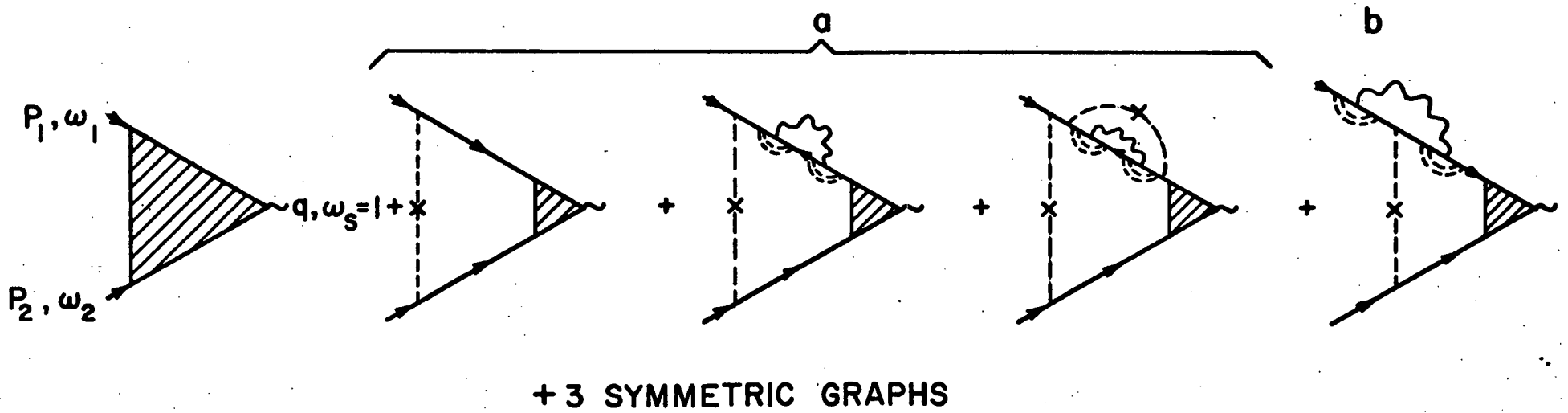


Fig. 2

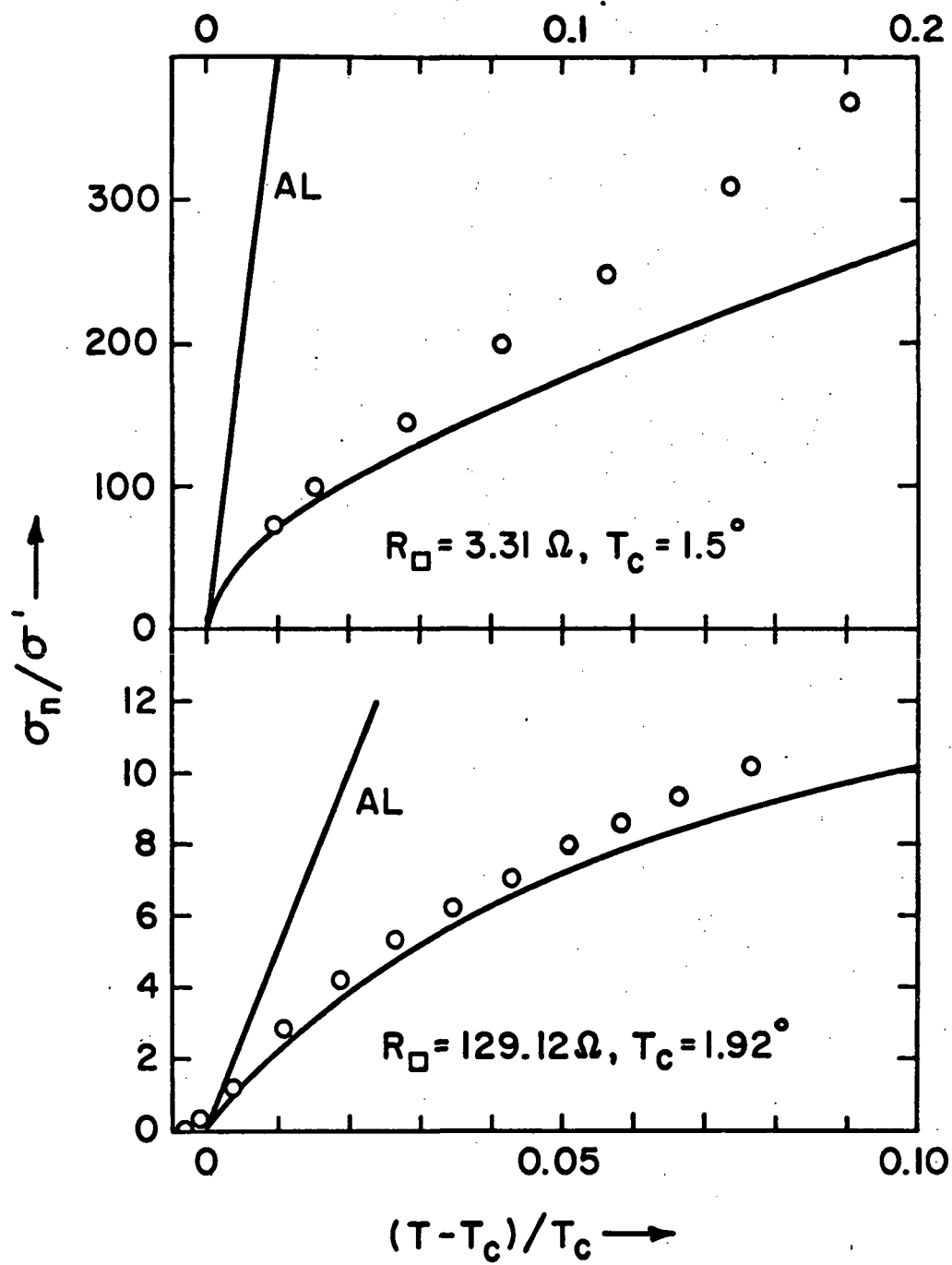


Fig. 3

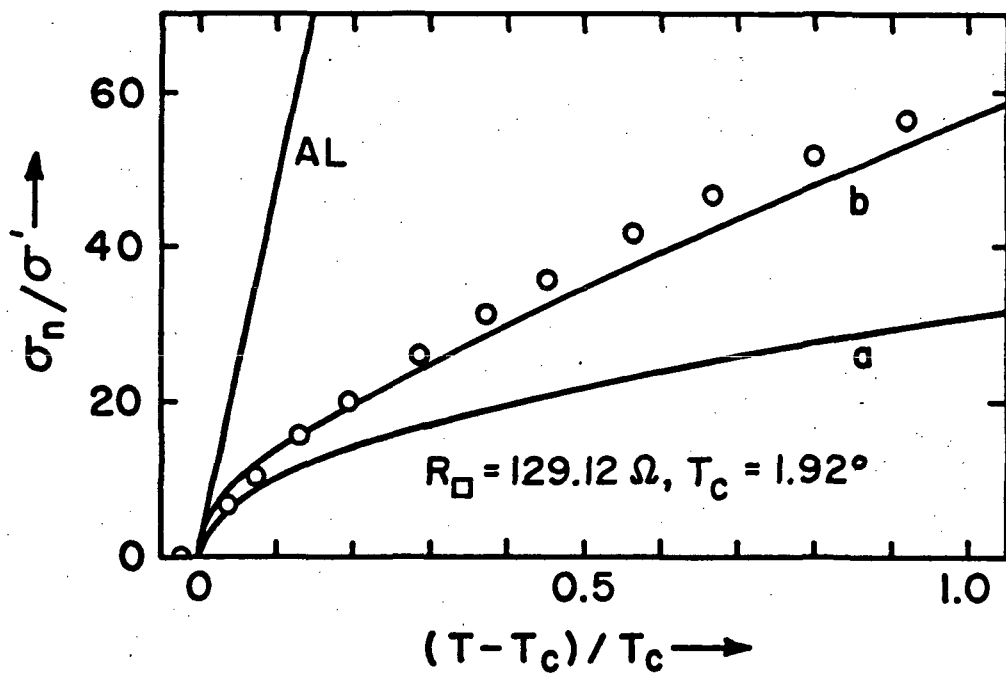


Fig. 4